AIAA JOURNAL
Vol. 30, No. 5, May 1992

Statistical Distribution of Frequency Response in Disordered Periodic Structures

G. Q. Cai* and Y. K. Lin†
Florida Atlantic University, Boca Raton, Florida 33431

A structure designed to be spatially periodic cannot be exactly periodic. The departure from exact periodicity is known as disorder, and it causes localization of normal modes and additional attenuation of wave motions in the structure not related to damping. The present investigation is directed at a possible adverse effect of disorder, namely, higher structural response near the point at which a dynamic excitation is applied than would occur in a perfectly periodic structure, thereby reducing structure safety and reliability. A systematic procedure is developed herein for the analysis of such an effect for a generic disordered periodic structure. In particular, the probability distribution of structural response is obtained by analysis and by Monte Carlo simulation, which is needed both for fundamental understanding of the effect and for predicting the reliability of a system. It is shown also that, given probability distributions of the disordered parameters of a structure, the mean and standard deviation of structural response can be obtained exactly for a damped randomly disordered periodic structure if the number of disordered cell units is not large and, approximately, if the number is large. Application of the procedure is illustrated by an example, and the results are compared with Monte Carlo simulations.

Introduction

MANY an engineering structure is designed to be an array of identically constructed units. These are known as periodic structures, and they possess some interesting dynamic properties. One of the properties is the existence of alternate wave-passage frequency bands and wave-stoppage frequency bands. If a periodic structure is infinitely long and undamped, then a disturbance can propagate indefinitely without attenuation if it is at a frequency within a wave-passage frequency band, or it decays in a short distance if it is at a frequency within a wave-stoppage frequency band. Extensive investigations of periodic structures are available in the literature, for example, Brillouin,[1] Miles,[2] Lin,[3-5] Lin and McDaniel,[6] and Mead.[7-10]

However, because of manufacturing and material irregularities, a structure designed to be periodic can never be perfectly periodic. Departure from perfect periodicity is known as disorder or mistuning, which may cause confinement of normal modes in a local region, and attenuation of wave propagation in wave-passage frequency bands, even if the structure is undamped. This is known as the localization effect, first predicted in a paper by Anderson[11] concerning transport of electrons in an atomic lattice, for which he shared a Nobel prize in physics.

The localization effect in disordered periodic structures (referred simply as disordered structures in the following) has also aroused considerable interest in the engineering research community. Deterministic analyses, conducted by Valero and Bendiksen,[12] Cornwell and Bendiksen,[13] and Pierre and his co-workers,[14-16] have shown that the normal modes that would be periodic in a perfectly periodic structure are localized in a small region when periodicity is disrupted. It is the modal localization that prevents a disturbance to propagate far away from the excitation point.

The average exponential rate at which a structural wave decays with respect to the wave propagation distance in a disordered structure is known as the localization factor. If a structure were exactly periodic, namely, any two adjoining substructures (cell units) were identical, then a structural wave would pass through the interface of every pair of adjoining units. On the other hand, in a disordered system, two adjoining units are generally different; therefore, some reflection generally takes place at the interfaces, and a total transmission is no longer possible. The localization factors due to disorder have been evaluated by Hodges and Woodhouse,[17] Pierre,[18] Kissel,[18] and Cai and Lin[20] using various perturbation schemes for the cases of either weak, moderate, or strong localization.

Both the localization of normal modes and wave attenuation suggest a possible energy concentration near the point at which an excitation is applied, causing a higher level of local dynamic response than would occur in a perfectly periodic structure. The problem appears to be even more interesting than wave decaying rate because a higher response level affects the structural safety and reliability adversely. Past investigations in this area have been related to bladed disks,[21-26] involving either deterministically disordered systems or small samples of randomly disordered systems. Conflicting results were reported from these studies. For example, Sogliero and Srinivasan[24] and Kaza and Kielb[21] found that disorder had a beneficial effect of reducing the forced response, whereas Ewins and Han[22] and MacBain and Whaley[23] showed that the opposite was true.

Analyses based on a deterministic case or small samples of cases are inadequate. A comprehensive understanding of the effects of disorder on free vibration and forced structural response can only be gained from truly stochastic analyses. Early stochastic analyses, in which the disordered physical quantities were treated as random variables, were carried out by Soong and Bogdanoff[27,28] for a chain of linear oscillators and by Lin and Yang[29,30] for multispan beams. In these works, perturbation schemes were employed to obtain statistical properties of natural frequencies, normal modes, and frequency response functions. It was found that, depending on the excitation frequency, the mean frequency response of a disordered beam could be either higher or lower than the value obtained without disorder. Another example of perturbation analysis was the work by Huang[25] on the mean and variance of the response amplitude of a mistuned bladed disk. The case of a two-span disordered beam with a torsional spring at the middle support was investigated by Hamade and Nikolaidis,[31] in which the well-known second-moment method of structural

Received Jan. 10, 1991; revision received July 22, 1991; accepted for publication July 31, 1991.

*Research Assistant, Center for Applied Stochastics Research.
†Schmidt Chair in Engineering and Director, Center for Applied Stochastics Research. Associate Fellow AIAA.

reliability was also employed to estimate the probability of failure for the system. The only analysis that focused on the probability density of the structural response was given by Sinha.[26] However, his method applies only to some specific disordered structures, not a generic disordered structure. Nor does it apply when the excitation frequency is near a resonant frequency, which is of the greatest practical interest.

In the present paper, a systematic procedure is developed for the analysis of a generic disordered structure. Such a procedure is clearly more desirable since it is not limited to a particular set of physical parameters, and the results so obtained will reveal the common features of an entire class of disordered structures. Furthermore, we will place special emphasis on the probability distribution of structural response, which is needed both for fundamental understanding of the effects of disorder and for predicting the reliability of a system. As a preliminary to the subsequent stochastic analysis, the frequency response of a deterministically disordered structure is first formulated by using the theory of wave propagation. This deterministic formulation is then "randomized" to obtain probabilistic and statistical properties of the frequency response. In particular, the probability density can be obtained by analysis for an undamped structure. Mean and variance can be obtained exactly by analysis for a damped structure if the number of cell units is small and approximately if the number is large. As a by-product, a procedure is devised to compute the limiting (or invariant) probability density of the phase difference between the right-going and left-going waves at the same location in an undamped disordered structure of semi-infinite length.

For illustration, numerical results are presented for a disordered multispan beam.

Wave Propagation in an Ideal Periodic Structure

Consider first an ideal periodic structure, consisting of N identical cell units that are connected sequentially in an array as shown in Fig. 1. The demarcation stations, which set the boundaries of individual cells, are numbered from left to right, beginning from station 1 and ending with station $N + 1$. Thus, stations n and $n + 1$ mark the boundaries of cell n. The state vectors at stations n and $n + 1$ are related as follows

$$\begin{Bmatrix} w(n+1) \\ f(n+1) \end{Bmatrix} = [T] \begin{Bmatrix} w(n) \\ f(n) \end{Bmatrix} \tag{1}$$

where each state vector consists of a p-dimensional subvector w of generalized displacements, and the corresponding p-dimensional subvector f of generalized forces, and $[T]$ is a $2p \times 2p$ transfer matrix associated with the nth cell. It is implied in Eq. (1) that the motion is timewise sinusoidal with a frequency ω. Then, the subvectors w and f are interpreted as complex amplitudes of the displacements and forces, respectively, and matrix $[T]$ is frequency dependent. For an ideal periodic structure, the transfer matrices associated with all cells are identical; therefore, the cell number n for the transfer matrix $[T]$ is not indicated in Eq. (1).

One well-known property shared by every transfer matrix is that its eigenvalues are reciprocal pairs. Thus, we can denote the eigenvalues of the ideal transfer matrix $[T]$ as $\lambda_1, \lambda_2, \ldots, \lambda_p$ and $\lambda_1^{-1}, \lambda_2^{-1}, \ldots, \lambda_p^{-1}$, where $|\lambda_1| \leq |\lambda_2| \leq \ldots \leq |\lambda_p| \leq 1$. The eigenvectors corresponding to these eigenvalues constitute a transformation matrix $[D]$, with which the state vectors in Eq. (1) are transformed to wave vectors as follows[32]

$$\begin{Bmatrix} w(i) \\ f(i) \end{Bmatrix} = [D] \begin{Bmatrix} \mu^r(i) \\ \mu^l(i) \end{Bmatrix}, \qquad (i = n,\ n+1) \tag{2}$$

where the subscript r or l associated with a wave vector indicates the direction of wave propagation, to be either right-going or left-going, and where matrix $[D]$ is normalized on the basis of unit energy flux.[33]

Substituting Eq. (2) into Eq. (1), one obtains

$$\begin{Bmatrix} \mu^r(n+1) \\ \mu^l(n+1) \end{Bmatrix} = [D]^{-1}[T][D] \begin{Bmatrix} \mu^r(n) \\ \mu^l(n) \end{Bmatrix} = [Q] \begin{Bmatrix} \mu^r(n) \\ \mu^l(n) \end{Bmatrix} \tag{3}$$

where $[Q]$ is also a transfer matrix, but it transfers wave vectors, instead of state vectors. This wave transfer matrix is clearly diagonal. In fact,

$$[Q] = [D]^{-1}[T][D] = \begin{bmatrix} \Lambda & 0 \\ 0 & \Lambda^{-1} \end{bmatrix} \tag{4}$$

where $\Lambda = \text{diag}\ (\lambda_1, \lambda_2, \ldots, \lambda_p)$. The diagonal form of this wave transfer matrix implies that no reflection occurs at the interface between two identical cells. In this context, a wave motion in a periodic structure is defined only for its magnitude at each boundary of each cell, disregarding details within the cell. This magnitude is, in fact, superposition of complicated component wave motions passing through a cell. In terms of such component waves, reflections do occur at the interface, as well as transmissions. However, their total effects at the interface should add up to transmission only.

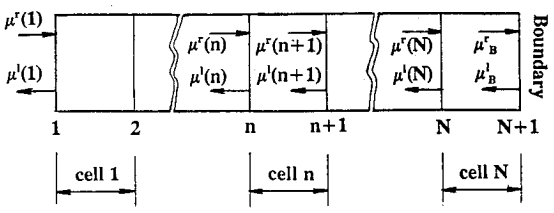

Fig. 1 Schematic of wave motions in an N-cell structure.

Deterministically Disordered Structure

If two adjoining cells are not identical, a wave motion impinging on their interface will not be totally transmitted, but it will be partially reflected back toward the reverse direction. Mathematically, the wave transfer matrix is no longer diagonal. We shall now investigate the case of a chain of disordered cells, assuming that their differences are known deterministically. Our main concern for the present investigation is the response localization, in contrast to our earlier work[20] in which the decay of wave propagation was the main objective.

For simplicity, we shall explore in detail a monocoupled chain, where only one generalized displacement is permitted at each cell-to-cell interface. In this case, the transfer matrices are 2×2, implying that only one type of wave motion can propagate through the chain, although two waves of the same type, one left-going and another right-going, are possible. The input to the chain is a sinusoidal force of frequency ω, acting at the left boundary of the first cell and with a complex amplitude $f(1)$. The output of interest is the steady-state displacement at the same location with a complex amplitude $w(1)$. It can be shown, by using Eq. (2), that the frequency response function $H(\omega)$ is given by

$$H(\omega) = \frac{w(1)}{f(1)} = \frac{d_{11}\mu^r(1) + d_{12}\mu^l(1)}{d_{21}\mu^r(1) + d_{22}\mu^l(1)} = \frac{d_{11}\eta(1) + d_{12}}{d_{21}\eta(1) + d_{22}} \tag{5}$$

where d_{ij} are elements of matrix $[D]$, which, for the present purposes, is chosen to be the transformation matrix associated with the ideal nondisordered cell, and $\eta(1)$ is the ratio of the right-going and left-going waves at the left boundary of the first cell, namely, $\eta(1) = \mu^r(1)/\mu^l(1)$. For a monocoupled chain, the symbols $w(1)$, $f(1)$, $\mu^r(1)$, and $\mu^l(1)$ in Eq. (5) are scalars.

For an interior cell, say cell n, we can deduce from Eq. (3)

$$\eta(n) = \frac{\mu^r(n)}{\mu^l(n)} = \frac{q_{12}(n) - \eta(n+1)q_{22}(n)}{\eta(n+1)q_{21}(n) - q_{11}(n)} \tag{6}$$

where $q_{ij}(n)$ are the elements of the wave transfer matrix $[Q(n)]$ for the nth cell, defined as

$$[Q(n)] = [D]^{-1}[T(n)][D] \tag{7}$$

In Eq. (7), the state transfer matrix $[T(n)]$ is computed on the basis of material and geometrical properties of the nth cell; it includes any possible disorders in the cell. The transformation matrix $[D]$, however, still corresponds to the ideal cell without disorder. It is of interest to note that Eq. (6) is a recursive relationship, which shows that $\eta(n)$ depends on $\eta(n+1)$ as well as the physical properties of the nth cell.

For the last cell at the right end of the chain,

$$\eta(N) = \frac{q_{12}(N) - \eta_B q_{22}(N)}{\eta_B q_{21}(N) - q_{11}(N)} \tag{8}$$

where η_B is the ratio of the right-going and left-going waves at the right boundary. However, η_B can be determined from the boundary condition. For example, if the right boundary of the chain is clamped, namely, $w_B = 0$, then $\eta_B = -d_{12}/d_{11}$; and if the boundary is free, namely, $f_B = 0$, then $\eta_B = -d_{22}/d_{21}$. Therefore, given a boundary condition at the right end of the chain, $\eta(N)$ depends on the physical properties of the end cell alone.

Equations (5–8) provide a simple way to calculate the frequency response function $H(\omega)$ for a disordered chain in which the physical properties are different from cell to cell. We begin by computing η_B for a specific boundary condition at the right end. We then determine progressively $\eta(N)$, $\eta(N-1), \ldots, \eta(1)$ using Eqs. (8) and (6). Finally, the frequency response function is obtained from Eq. (8). The scheme is numerically efficient, thus, it can be applied to a large number of such chains for the purpose of Monte Carlo simulation.

It is of interest to examine the limiting case of an ideal periodic structure without disorder. In such a case, $q_{11}(n) = \lambda$, $q_{22} = \lambda^{-1}$, $q_{12}(n) = q_{21}(n) = 0$, independent of n. Then application of Eqs. (6) and (8) yields $\eta(1) = \eta_B \lambda^{-2N}$, whereupon

$$H(\omega) = \frac{\eta_B \lambda^{-2N} d_{11} + d_{12}}{\eta_B \lambda^{-2N} d_{21} + d_{22}} \tag{9}$$

Since damping generally exists in a structural system, $|\lambda| < 1$. Thus, $H(\omega)$ tends to d_{12}/d_{22} for a long ideal periodic structure, independent of the boundary condition at the far end.

Undamped Randomly Disordered Structure

Since disorder in a periodic structure has a similar effect as damping on wave propagation, namely, it gives rise to an exponential spatial decay of the wave amplitude along the chain, damping is often neglected if the objective of an analysis is to estimate the effect due to disorder alone.[12–20] Furthermore, an analytical solution for an undamped structural model is often easier to obtain and it may provide clearer insight into the physical problem.

Refer to a typical inner cell, say the nth cell of an undamped disordered N-cell chain. Energy conservation requires that

$$|\mu^r(n)|^2 + |\mu^l(n+1)|^2 = |\mu^l(n)|^2 + |\mu^r(n+1)|^2 \tag{10}$$

The left- and right-hand sides of Eq. (10) represent, respectively, the average energy in-flow and energy out-flow of the cell within one period of time $2\pi/\omega$. If, furthermore, no energy dissipation mechanism exists at the right boundary of the chain, then $|\mu_B^r|^2 = |\mu_B^l|^2$. It follows that $|\mu^r(n)|^2 = |\mu^l(n)|^2$ and $|\eta(n)| = 1$, which implies that $\eta(n)$ can be expressed as

$$\eta(n) = e^{i\theta(n)} \tag{11}$$

where $\theta(n)$ is purely real; it represents the phase difference between the two waves $\mu^r(n)$ and $\mu^l(n)$. This is a very significant simplification since the complex random variable $\eta(n)$ can now be described by a real random variable $\theta(n)$ alone.

With this simplification, Eqs. (5), (6), and (8) are reduced to

$$H = \frac{e^{i\theta(1)} d_{11} + d_{12}}{e^{i\theta(1)} d_{21} + d_{22}} \tag{12}$$

$$e^{i\theta(n)} = \frac{q_{12}(n) - e^{i\theta(n+1)} q_{22}(n)}{e^{i\theta(n+1)} q_{21}(n) - q_{11}(n)}; \quad n = N-1, \ldots, 2, 1 \tag{13}$$

$$e^{i\theta(N)} = \frac{q_{12}(N) - e^{i\theta_B} q_{22}(N)}{e^{i\theta_B} q_{21}(N) - q_{11}(N)} \tag{14}$$

Each of the random parameters in a disordered cell unit may be represented by a mean (or the nominal design value) plus a random variable with zero mean. For cell n, these random variables may be denoted by a vector $\boldsymbol{x}(n)$; namely, $\boldsymbol{x}(n) = \{x_1(n), x_2(n), \ldots, x_k(n)\}^T$. Being functions of the disordered parameters, $q_{ij}(n)$ may be denoted by

$$q_{ij}(n) = q_{ij}[\boldsymbol{x}(n)] \tag{15}$$

It is reasonable to assume that $x_j(n)$ for each j but different n are independent and identically distributed random variables and that they form an ergodic sequence if the disordered chain is infinitely long. Equations (12–14) describe the functional dependences of random variables H and $\theta(n)$ ($n = 1, 2, \ldots, N$); thus, their probability density functions can be obtained as follows

$$p[\theta(N)] = \int p[\boldsymbol{x}(N)] \left| \frac{\partial x_1(N)}{\partial \theta(N)} \right| \mathrm{d}x_2(N) \ldots \mathrm{d}x_k(N) \tag{16}$$

$$p[\theta(n)] = \int p[\theta(n+1)] p[\boldsymbol{x}(n)] \left| \frac{\partial \theta_1(n+1)}{\partial \theta(n)} \right| \mathrm{d}\boldsymbol{x}(n) \tag{17}$$

$$p[z] = p[\theta(1)] \left| \frac{\mathrm{d}\theta(1)}{\mathrm{d}z} \right| \tag{18}$$

where $z = |H|$ and each $p[\,]$ denotes a probability density. In obtaining Eq. (17), use has been made of the independence of the two random variables $\theta(n+1)$ and $\boldsymbol{x}(n)$ due to the fact that $\eta(n+1)$, hence, $\theta(n+1)$, is only related to random vectors $\boldsymbol{x}(n+1), \boldsymbol{x}(n+2), \ldots, \boldsymbol{x}(N)$, as can be seen from the recursive relationship, Eq. (6).

For a disordered chain with a finite total length, we evaluate $p[\theta(n)]$ from $n = N$ to $n = 1$ by numerically integrating Eqs. (16) and (17) recursively and then obtain $p(z)$ from Eq. (18). If each cell unit possesses k disordered parameters, the integrals in Eqs. (16) and (17) are $(k-1)$-fold and k-fold, respectively.

It is conceptually illuminating to consider the case of a semi-infinite disordered chain; namely, when $N \to \infty$. In this case, $p[\theta(n)]$ becomes independent of n, for any finite n. In other words, the probability distribution for the phase difference between the right-going and left-going waves becomes invariant in a semi-infinite disordered chain. The existence of such an invariant probability density (also referred to as invariant measure) has been proved by Furstenberg[34] and is known in the mathematics literature as Furstenberg's theorem and in the physics literature as the Dyson-Schmidt self-consistency condition. An explicit analytical expression for the invariant measure $p(\theta)$ is generally difficult to obtain; however, it must satisfy the relation

$$\{p[\theta(n)]\}_{\theta(n)=\theta} = \left\{ \int p[\theta(n+1)] \times p[\boldsymbol{x}(n)] \left| \frac{\partial \theta(n+1)}{\partial \theta(n)} \right| \mathrm{d}\boldsymbol{x}(n) \right\}_{\theta(n)=\theta} = \{p[\theta(n+1)]\}_{\theta(n+1)=\theta} \tag{19}$$

For specific cases, it can be calculated approximately using a perturbation approach, as shown later in an example.

Of course, a semi-infinite disordered chain does not actually exist. However, the invariant probability distribution, obtained for a semi-infinite chain, is a good approximation for at least the first several cells, if the entire chain is sufficiently long. If such an invariant probability can be found, then the probability density $p(z)$ for the response amplitude can be computed directly from Eq. (18).

Damped Randomly Disordered Structure

If damping in the structure is taken into consideration, then each complex wave ratio η must be described in terms of two real random variables, which may be chosen to be the amplitude $|\eta|$ and the phase difference θ. In principle, the joint probability of $|\eta|$ and θ for every cell can still be calculated using the probability theory and Eqs. (6) and (8); however, the required computations can be very time consuming in order to achieve a sufficient level of accuracy. Interestingly, a Monte Carlo simulation procedure making use of the recurrence relationship Eq. (6) is rather efficient for this problem. With a large enough sample size, the simulated distribution can be quite accurate. In general, a larger sample size is required for the computation of probability densities than what is needed for the mean or mean square values.

If a randomly disordered chain contains only a small number of cells, then the mean and mean-square values of the response magnitude can be obtained exactly. For an N-cell chain, we may write

$$\begin{Bmatrix} \mu_B^r \\ \mu_B^l \end{Bmatrix} = [Q(N,1)] \begin{Bmatrix} \mu^r(1) \\ \mu^l(1) \end{Bmatrix} \tag{20}$$

where $[Q(N,1)]$ is the wave transfer matrix for the entire chain, obtainable as

$$[Q(N,1)] = [Q(N)][Q(N-1)] \ldots [Q(2)][Q(1)] \tag{21}$$

It follows from the definition of wave ratios η,

$$\eta(1) = \frac{q_{12}(N,1) - \eta_B q_{22}(N,1)}{\eta_B q_{21}(N,1) - q_{11}(N,1)} \tag{22}$$

Combining Eqs. (5) and (22),

$$H = \frac{d_{11}(q_{12} - \eta_B q_{22}) + d_{12}(\eta_B q_{21} - q_{11})}{d_{21}(q_{12} - \eta_B q_{22}) + d_{22}(\eta_B q_{21} - q_{11})} \tag{23}$$

where the arguments $(N,1)$ for each q_{ij} are omitted for simplicity. In Eq. (23), d_{ij} and η_B are constants, and the $q_{ij}(N,1)$ are functions of the random vectors $x(1), x(2), \ldots, x(N)$; therefore, H is also a function of $x(1), x(2), \ldots, x(N)$. The mean and mean square values of $z = |H|$ are then obtained from ensemble averaging; namely,

$$E[z] = \int |H| p[x(1)] \ldots p[x(N)]\, dx(1)\, dx(N) \tag{24}$$

$$E[z^2] = \int |H|^2 p[x(1)] \ldots p[x(N)]\, dx(1)\, dx(N) \tag{25}$$

The domain of the $N \times k$-fold integrations in Eqs. (24) and (25) is a super-rectangle; they can be carried out numerically without difficulty provided that $N \times k$ is not too large. The product form $p[x(1)] \ldots p[x(N)]$ implies that $x(1), \ldots, x(N)$ are mutually independent, and all $p[x(n)]$ are of the same form under the assumption of identical distribution.

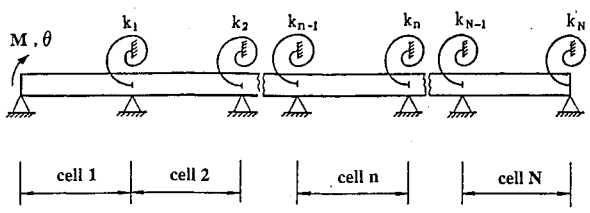

Fig. 2 Multispan beam.

When the number of cells in a disordered chain is very large, the previously mentioned numerical integration scheme is no longer practical. In this case, however, the wave ratio $\eta(1)$ is essentially affected by those cells nearer to the excitation point and is least affected by those near the far end. By taking only the first m cells into account, we obtain, analogous to Eq. (22),

$$\eta(1) \approx \frac{q_{12}(m,1) - \eta(m+1) q_{22}(m,1)}{\eta(m+1) q_{21}(m,1) - q_{11}(m,1)} \tag{26}$$

For small disorders, it can be shown that, approximately, $q_{22}(m,1)$ increases as λ^{-m}, $q_{11}(m,1)$ decreases as λ^m, and $q_{12}(m,1)$ and $q_{21}(m,1)$ increases as $\lambda^{-m/2}$, where λ is the smaller of the two eigenvalues of the nondisordered transfer matrix $[T]$, and $|\lambda| < 1$. In addition, $|\eta|$ is expected to be greater than 1, although its precise value is determined by the system properties. This is due to the fact that, with an excitation applied at the left end, the energy flow to the right is always greater than the energy flow to the left at any station along the chain. Consequently, Eq. (26) may be approximated as

$$\eta(1) \approx -\frac{q_{22}(m,1)}{q_{21}(m,1)} \tag{27}$$

if m is sufficiently large. The size of m depends on the magnitude of damping; the smaller the damping, the larger size of m is required. In practice, m can be selected by trial and error. A further increase of m is no longer warranted when such an increase does not produce significantly different results.

On the basis of the approximate expression, Eq. (27), the mean and mean-square values of the response amplitude z are obtained as

$$E[z] = \int \left| \frac{d_{12} q_{21}(m,1) - d_{11} q_{22}(m,1)}{d_{22} q_{21}(m,1) - d_{21} q_{22}(m,1)} \right| \times p[x(1)] \ldots p[x(m)]\, dx(1) \ldots dx(m) \tag{28}$$

$$E[z^2] = \int \left| \frac{d_{12} q_{21}(m,1) - d_{11} q_{22}(m,1)}{d_{22} q_{21}(m,1) - d_{21} q_{22}(m,1)} \right|^2 \times p[x(1)] \ldots p[x(m)]\, dx(1) \ldots dx(m) \tag{29}$$

Example

For illustration purposes, this theory will now be applied to an example shown in Fig. 2; namely, an Euler-Bernoulli beam on evenly spaced hinge supports and, with the exception of the first support, a torsional spring is added at each support. To bring out basic features of the problem without being obscured by unnecessary complexities, only the torsional spring stiffnesses are assumed to be random, and they are described by

$$k_n = k_0[1 + x(n)], \qquad n = 1, 2, \ldots \tag{30}$$

where k_0 is the average k_n, and $x(n)$ are independent and identically distributed random variables with zero means. For numerical computation, $x(n)$ are further assumed to be uniformly distributed between $-\sqrt{3}\sigma$ and $\sqrt{3}\sigma$, where σ is the standard deviation. The other physical parameters are treated as being deterministic, including the distances between two neighboring supports l, the mass of the beam per unit length M, and the bending rigidity of the beam EI. The structural damping is introduced by adding an imaginary part to the Young's modulus E; namely, $E = E_0(1 + i\zeta\, \mathrm{sgn}\omega)$, where ζ is called the loss factor.

A typical cell unit is chosen to include a beam element between two neighboring supports and the entire torsional spring on its right. The torsional spring on the left is treated as belonging to the preceding cell. The generalized displacement and the corresponding generalized force at each cell-to-cell interface are the rotation angle and the bending moment, respectively. Accordingly, the transfer matrix for the nth cell is given by

$$[T(n)] = \begin{bmatrix} \beta & \alpha/\nu \\ -\dfrac{\nu(1-\beta^2)}{\alpha} + \dfrac{\beta}{\delta}[1+x(n)] & \beta + \dfrac{\alpha}{\delta\nu}[1+x(n)] \end{bmatrix} \tag{31}$$

where $\delta = EI/lk_0$, $\nu = l(\omega^2 M/EI)^{1/4}$, ω is the frequency,

$$\alpha = \frac{\cosh \nu \cos \nu - 1}{\sinh \nu - \sin \nu} \tag{32}$$

and

$$\beta = \frac{\sinh \nu \cos \nu - \cosh \nu \sin \nu}{\sinh \nu - \sin \nu} \tag{33}$$

The ideal transfer matrix $[T]$ is obtained by letting $x(n) = 0$ in Eq. (31). Its eigenvalues are the two roots of the equation

$$\lambda^2 = \left(2\beta + \frac{\alpha}{\delta\nu}\right)\lambda + 1 = 0 \tag{34}$$

The following physical constants were used in the numerical calculations: $l = 0.1051$ m, $M = 1.8043$ kg/m, $E_0I = 0.3134$ N-m^2, and $\delta_0 = E_0I/k_0 = 0.1$. The results are described in the following.

Undamped Case

Consider first the case in which the structure is undamped and the excitation frequency ω falls within one of the wave-passage frequency bands. Then the two eigenvalues of $[T]$ can be represented by $e^{\pm i\psi}$, where ψ is purely real and is obtainable from[5]

$$\cos \psi = \beta + \frac{\alpha}{2\delta_0\nu_0}, \qquad \left|\beta + \frac{\alpha}{2\delta\nu_0}\right| \le 1 \tag{35}$$

where

$$\nu_0 = l\left(\frac{\omega^2 M}{E_0 I}\right)^{1/4}$$

The probability densities of the wave phase difference $\theta(1)$ and the frequency response amplitude, normalized with respect to the reference value z_p of the corresponding ideal periodic system and computed from Eqs. (16–18), are shown in Figs. 3a, 3b, 4a, and 4b. In Figs. 3a and 3b, four different cases corresponding to four total cell numbers, $N = 5$, 15, 30, and 100, are plotted, with the standard deviation of the disorder parameter x fixed at $\sigma = 0.1$. In Figs. 4a and 4b, the cell number is fixed at $N = 30$, but the standard deviation σ is chosen to be either 0.05, 0.1, or 0.2. It is seen that an increase of either the cell number or the level of disorder causes both $p[\theta(1)]$ and $p(z/z_p)$ to become more extended and flatter. In both the cases of $N = 100$ in Fig. 3a and $\sigma = 0.2$ in Fig. 4a, the distribution of the wave phase difference $\theta(1)$ becomes almost uniform within $(-\pi, \pi)$. It should be pointed out that the dispersion of a system parameter, characterized by σ, is usually small in practical problems. However, the cases of large σ are also illustrated herein to show the general trends.

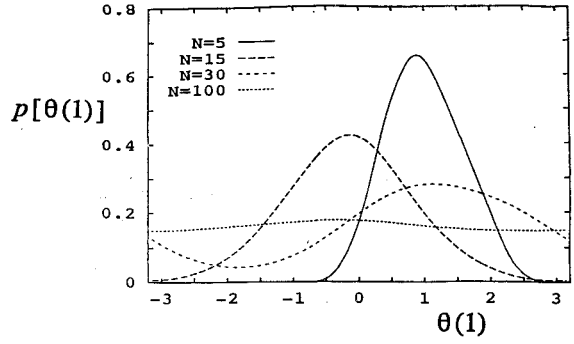

a) Probability density of wave phase difference $\theta(1)$

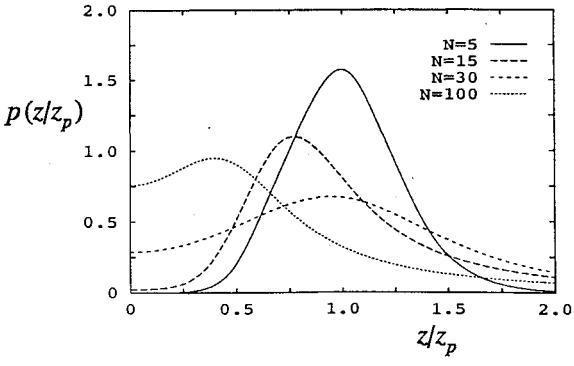

b) Probability density of nondimensional frequency response magnitude z/z_p

Fig. 3 Undamped disordered beams with different numbers of span: $\sigma = 0.1$; $\omega = 250$ rad/s.

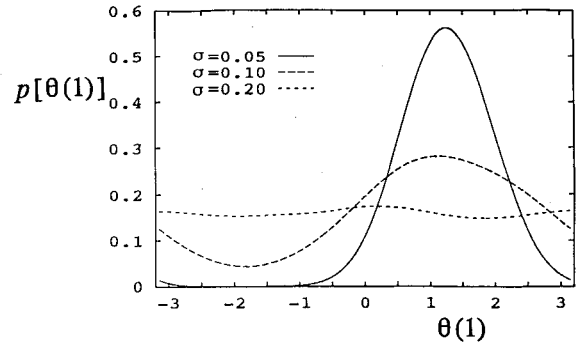

a) Probability density of wave phase difference $\theta(1)$

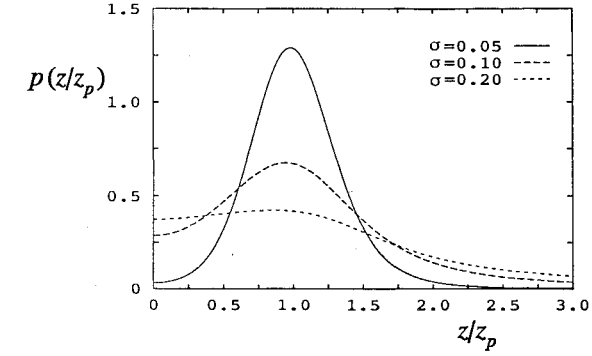

b) Probability density of nondimensionalized frequency response magnitude z/z_p

Fig. 4 Undamped 30-span beams with different levels of disorder:

Invariant Probability of Wave Phase Difference

The invariant probability density of the wave phase difference for a semi-infinite disordered chain must satisfy Eq. (19). For the present multispan beam, Eq. (19) has the following specific form

$$[p(\theta')_{\theta'=\theta} = \left\{\frac{1}{2\sqrt{3}\sigma}\int_{-\sqrt{3}\sigma}^{\sqrt{3}\sigma}\left|\frac{\partial\theta}{\partial\theta'}\right| p[\theta(\theta', x)]\, dx\right\}_{\theta'=\theta} = p(\theta) \tag{36}$$

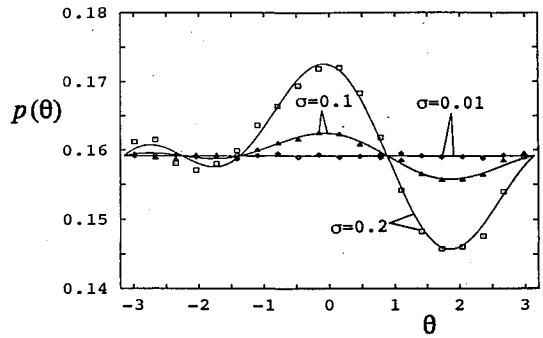

Fig. 5 Invariant probability density of wave phase difference θ, undamped semi-infinite disordered beams: $\omega = 250$ rad/s.

where θ' and θ take the places of $\theta(n)$ and $\theta(n+1)$, respectively, in Eq. (19), where

$$\left|\frac{\partial\theta}{\partial\theta'}\right| = G(\theta',x) = \{1 - 2A_0x\sin(\theta' + 2\psi) + 2A_0^2x^2[1 + \cos(\theta' + 2\psi)]\}^{-1} \quad (37)$$

and where $\theta(\theta',x)$ represents the following implicit relations:

$$\sin\theta = \{\sin(\theta' + 2\psi) - 2A_0x[1 + \cos(\theta' + 2\psi)]\}G(\theta',x) \quad (38a)$$

$$\cos\theta = \{\cos(\theta' + 2\psi) + 2A_0x\sin(\theta' + 2\psi) - 2A_0^2x^2[1 + \cos(\theta' + 2\psi)]\}G(\theta',x) \quad (38b)$$

with $A_0 = \alpha/(2\delta_0\nu_0\sin\psi)$. Equations (37) and (38) are derived from the functional relationship between $\theta(n)$ and $\theta(n+1)$ given in Eq. (13).

Since $|x|$ is bounded by $\sqrt{3}\sigma$, a perturbation procedure, applicable when $|A_0\sigma|$ is small, can be devised as follows. Let

$$p(\theta) = \frac{1}{2\pi} + \sum_{j=1}^{\infty}(C_j\sin j\theta + D_j\cos j\theta) \quad (39)$$

where

$$C_j = C_{j0} + C_{j1}A_0\sigma + C_{j2}(A_0\sigma)^2 + \ldots \quad (40a)$$

$$D_j = D_{j0} + D_{j1}A_0\sigma + D_{j2}(A_0\sigma)^2 + \ldots \quad (40b)$$

In Eq. (39), $p(\theta)$ can be expanded into a Fourier series because it is a periodic function with a period 2π. The constant term in this expression is known to be $1/2\pi$; otherwise, the normalization condition for $p(\theta)$ will not be satisfied.

Substituting Eqs. (39) and (40) into Eq. (36) and equating terms of the same power in $A_0\sigma$, the coefficients C_{jk} and D_{jk} can be obtained. The final expressions for $p(\theta)$ are

$$p(\theta) = \frac{1}{2\pi}\left\{1 + A_0^2\sigma^2\frac{\sin(\theta+\psi)}{\sin\psi}\left[1 + \frac{\cos(\theta+\psi)}{\cos\psi}\right]\right\} + 0(A_0\sigma)^4$$

$$\cos 2\eta\psi \neq 1, \qquad -\pi \leq \theta \leq \pi \quad (41)$$

This perturbation scheme is not applicable when $\cos 2\eta\psi = 1$.

Figure 5 depicts the computed approximate invariant measure $p(\theta)$ for the cases $\sigma = 0.01$, 0.1, and 0.2. The results are in good agreement with those obtained from Monte Carlo simulations, also shown in the figure as squares, triangles, and diamonds. The simulations were carried out according to Eqs. (8) and (6), starting from the right boundary. The distribution of θ became essentially invariant after 1000 cells and the simulation results shown in Fig. 5 correspond to a smoothed histogram obtained for the subsequent 10^6 cells. A chain of 10^6 cells is practically ergodic, and a single sample calculation is found to be adequate.

It is of interest to note that, for $\sigma = 0.2$, the invariant $p(\theta)$ for a semi-infinite chain shown in Fig. 5 is nearly the same as that of $p[\theta(1)]$ for a 30-cell chain shown in Fig. 4a if they were plotted in the same vertical scale. This means that, with $\sigma = 0.2$, a 30-cell chain behaves like a semi-infinite chain, which is not the case with $\sigma = 0.1$ and with $\sigma = 0.05$.

The approximate invariant measure $p(\theta)$ obtained earlier was then used to determine the probability density $p(z/z_p)$ for the normalized response amplitude for a semi-infinite disordered beam. The results are shown in Fig. 6 for $\sigma = 0.02$, 0.05, 0.1, and 0.2. The large differences in the level of disorder do not cause a significant spread of the results, suggesting that the dominant factor here is the infinite number of cells.

Effects of Damping

As indicated earlier, the Monte Carlo simulation procedure is efficient for computing samples of frequency response. Figure 7 shows the simulation results of $p(z/z_p)$ for a 20-span disordered beam with $\sigma = 0.1$ and $\zeta = 0$, 0.01, 0.05, and 0.1. The results for $\zeta = 0$ were also verified by comparing with the analytical results for undamped systems. It is found that damping has a significant effect on $p(z/z_p)$. It reduces the range over which the value of the frequency response is distributed. The higher the damping, the more closely a disordered system behaves like a nondisordered system. Therefore, damping is beneficial because it reduces not only the response level but also the likelihood for the response to reach a much higher value.

Exact values for the mean and the standard deviation of z/z_p were calculated for a six-span disordered beam with different damping levels by numerically integrating Eqs. (24) and (25). The results are shown in Figs. 8a and 8b along with the Monte Carlo simulation results. Again, damping reduces both the values of the mean and the standard deviation of the response, consistent with earlier conclusions on the probability density of disordered structure.

For a disordered beam with a large number of spans, the mean and mean-square values of the frequency response mag-

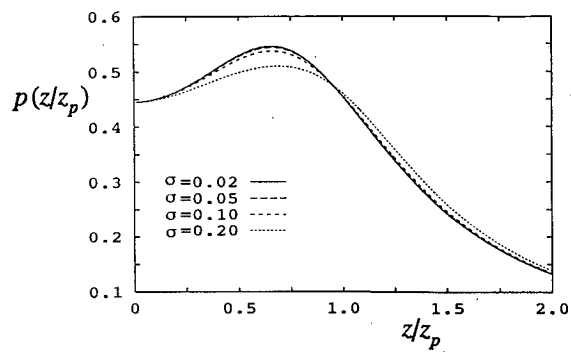

Fig. 6 Probability density of nondimensional frequency response magnitude z/z_p for undamped semi-infinite beams with different levels of disorder: $\omega = 250$ rad/s.

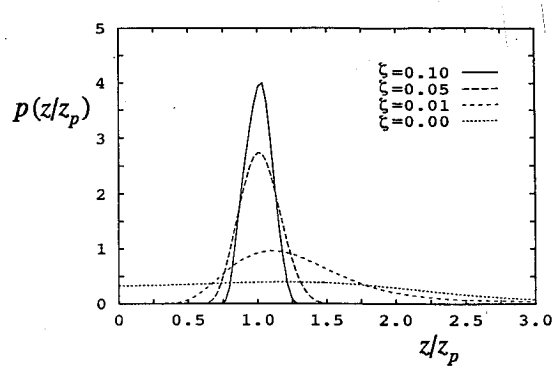

Fig. 7 Probability density of nondimensional frequency response magnitude, 20-span disordered beams with different levels of damping: $\sigma = 0.01$; $\omega = 250$ rad/s.

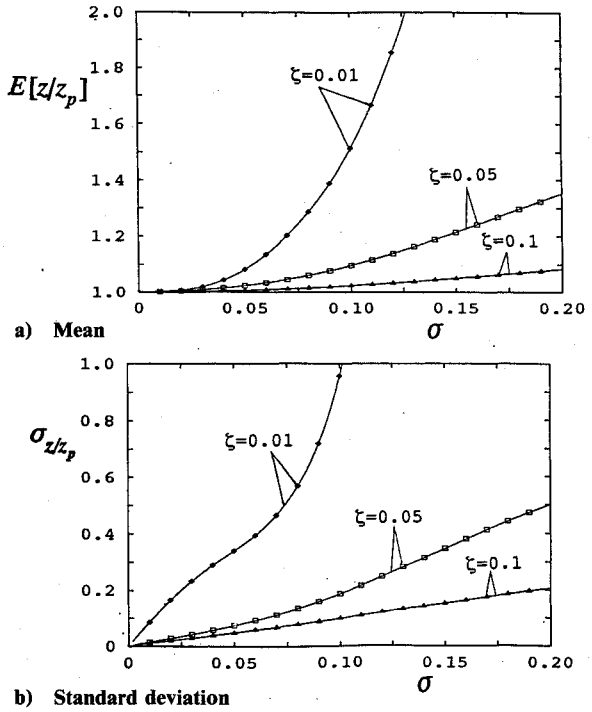

a) Mean

b) Standard deviation

Fig. 8 Mean and standard deviation of nondimensionalized frequency response magnitude, six-span disordered beams with different levels of damping: $\omega = 250$ rad/s.

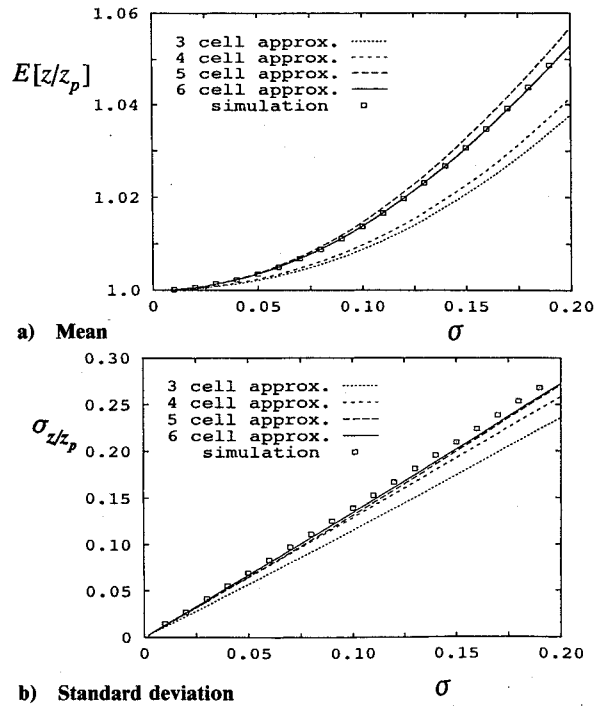

a) Mean

b) Standard deviation

Fig. 9 Mean and standard deviation of nondimensionalized frequency response magnitude, damped disordered beam with large number of cells: $\zeta = 0.05$; $\omega = 250$ rad/s.

nitude can be obtained approximately from Eqs. (28) and (29) by taking a smaller number of spans into consideration. Figures 9a and 9b show such approximate results as well as the Monte Carlo simulation results. For the case $\zeta = 0.05$, a six-cell approximation was found to be adequate, and the analytical results practically coincide with the simulation results when 40 or more spans were included in each sample. In other words, a six-cell approximation formula is adequate for a chain of 40 cells or longer for $\zeta \geq 0.05$. Of course, more cells must be taken into consideration for lower damping cases.

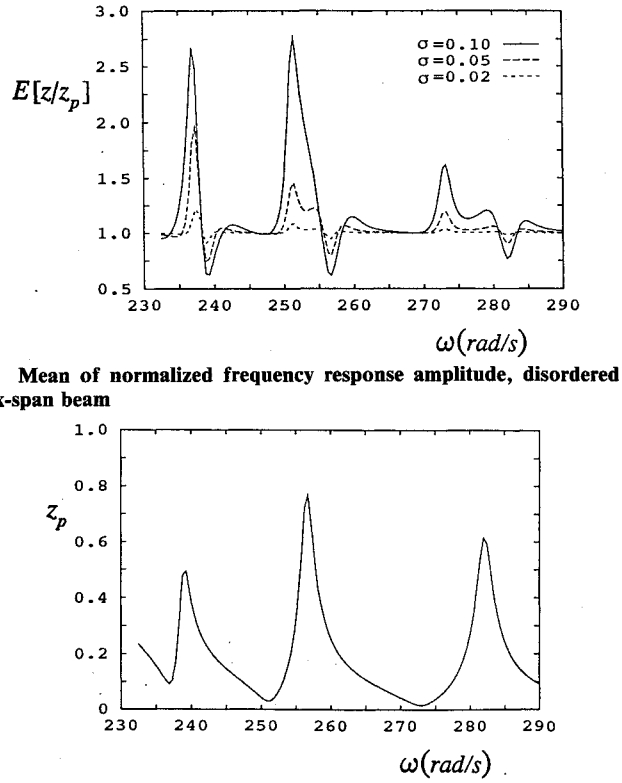

a) Mean of normalized frequency response amplitude, disordered six-span beam

b) Frequency response amplitude, perfectly six-span periodic beam

Fig. 10 Comparison of frequency response magnitudes between disordered and nondisordered six-span beams: $\zeta = 0.01$.

The results shown in Figs. 3–9 have been obtained for one single excitation frequency $\omega = 250$ rad/s, which is located within the first wave-passage frequency band. It is reasonable to expect that different results will be obtained at different frequencies. In Fig. 10a, the exact mean values of z/z_p are plotted vs frequencies within the lower half of the first wave-passage frequency band for a six-span disordered beam with a loss factor $\zeta = 0.01$. The magnitudes of the frequency response for the corresponding perfectly periodic structure are depicted in Fig. 10b for reference. The mean frequency response of a disordered system is seen to be very sensitive to the excitation frequency; it is much less than that of the perfectly periodic system if the excitation frequency is near a resonant frequency of the perfect periodic structure. This is to be expected since disorder causes a shift of the resonant frequency. On the other hand, at those frequencies where the magnitude of the frequency response of the perfectly periodic system reaches its local minimum, the mean value of z/z_p is greater than 1, indicating an increase of the average response level.

Concluding Remarks

The procedure developed herein for calculating the frequency response of a deterministically disordered periodic structure provides a convenient framework with which randomly disordered structures can be investigated by analysis as well as by Monte Carlo simulation. The recursive nature of the procedure makes the computations efficient. The key recursive variable, the wave ratio η, is restricted in magnitude within a certain range, guaranteeing the accuracy of the computed results.

Some important characteristics of a disordered structure have been observed from the computed results. The shape of the probability distribution of the frequency response magnitude of a randomly disordered structure indicated the relative likelihood that the magnitude can be either higher or lower than that of the corresponding ideally periodic structure. The number of disordered cells and the level of disorder play a

similar role in spreading the frequency response, and an increase in either one of the two leads to a larger standard deviation of the response. Finally, damping is shown to be beneficial in two ways; namely, reducing the response level and the likelihood for the response to reach a much higher value.

Acknowledgments

This paper is prepared under Grant AFOSR-88-0005 from the Air Force Office of Scientific Research, Air Force Systems Command, USAF, monitored by Spencer Wu. We acknowledge the help from one of the reviewers for this paper, who provided the information about Refs. 35 and 36, in which a similar ratio of the right-going and left-going waves, termed state ratio, was used in the analysis.

References

[1]Brillouin, L., *Wave Propagation in Periodic Structures,* Dover, New York, 1953.

[2]Miles, J. W., "Vibration of Beams on Many Supports," *Journal of the Engineering Mechanics Division, ASCE,* Vol. 82, No. EM1, Jan. 1956, pp. 1-9.

[3]Lin, Y. K., "Free Vibration of Continuous Skin-Stringer Panels," *Journal of Applied Mechanics,* Vol. 27, No. 4, Dec. 1960, pp. 669-676.

[4]Lin, Y. K., "Stresses in Continuous Skin-Stringer Panels under Random Loading," *Journal of Aero/Space Sciences,* Vol. 29, No. 1, Jan. 1962, pp. 67-86.

[5]Lin, Y. K., "Free Vibration of Continuous Beams on Elastic Supports," *Journal of Mechanical Science,* Vol. 4, Sept.-Oct. 1962, pp. 409-423.

[6]Lin, Y. K., and McDaniel, T. J., "Dynamics of Beam-Type Periodic Structures," *Journal of Engineering for Industry,* Vol. 91, Nov. 1969, pp. 1133-1141.

[7]Mead, D. J., "Free Wave Propagation in Periodically-Supported Infinite Beam," *Journal of Sound and Vibration,* Vol. 11, No. 2, 1970, pp. 181-197.

[8]Mead, D. J., "A General Theory of Harmonic Wave Propagation in Linear Periodic Systems with Multiple Coupling," *Journal of Sound and Vibration,* Vol. 27, No. 2, 1973, pp. 235-260.

[9]Mead, D. J., "Wave Propagation and Natural Modes in Periodic Systems: I. Mono-Coupling System, II. Multi-Coupled Systems, With and Without Damping," *Journal of Sound and Vibration,* Vol. 40, No. 1, 1975, pp. 1-39.

[10]Mead, D. J., and Markus, S., "Coupled Flexural-Longitudinal Wave Motion in Periodic Beams," *Journal of Sound and Vibration,* Vol. 90, No. 1, 1983, pp. 1-24.

[11]Anderson, P. W., "Absence of Diffusion in Certain Random Lattices," *Physical Review,* Vol. 109, No. 5, 1958, pp. 1492-1505.

[12]Valero, N. A., and Bendiksen, O. O., "Vibration Characteristics of Mistuned Shrouded Blade Assemblies," *Journal of Engineering for Gas Turbines and Power,* Vol. 108, No. 2, 1986, pp. 293-299.

[13]Cornwell, P. J., and Bendiksen, O. O., "Localization of Vibrations in Large Space Reflectors," AIAA Paper 87-0949, April 1987; also, *Proceedings of 28th AIAA/ASME/ASCE/AHS Structures, Structural Dynamics and Materials Conference,* Monterey, CA, pp. 925-935.

[14]Pierre, C., and Dowell, E. H., "Localization of Vibrations by Structural Irregularity," *Journal of Sound and Vibration,* Vol. 114, No. 3, 1987, pp. 549-564.

[15]Pierre, C., Tang, D. M., and Dowell, E. H., "Localized Vibrations of Disordered Multispan Beams: Theory and Experiment," *AIAA Journal,* Vol. 25, No. 9, 1987, pp. 1249-1257.

[16]Pierre, C., and Cha, P. D., "Strong Mode Localization in Nearly Periodic Disordered Structures," *AIAA Journal,* Vol. 27, No. 2, 1989, pp. 227-241.

[17]Hodges, C. H., and Woodhouse, J., "Vibration Isolation from Irregularity in a Nearly Periodic Structure: Theory and Measurements," *Journal of the Acoustical Society of America,* Vol. 74, No. 3, 1983, pp. 894-905.

[18]Pierre, C., "Weak and Strong Vibration Localization in Disordered Structures: A Statistical Investigation," *Journal of Sound and Vibration,* Vol. 139, No. 1, 1990, pp. 111-132.

[19]Kissel, G. J., "Localization in Disordered Periodic Structures," Ph.D. Dissertation, Massachusetts Inst. of Technology, Cambridge, MA, Feb. 1988.

[20]Cai, G. Q., and Lin, Y. K., "Localization of Wave Propagation in Disordered Periodic Structures," *AIAA Journal,* Vol. 29, No. 3, pp. 450-456.

[21]Kaza, K. R. V., and Kielb, R., "Flutter and Response of a Mistuned Cascade in Incompressible Flow," *AIAA Journal,* Vol. Vol. 20, No. 8, 1982, pp. 1120-1127.

[22]Ewins, D. J., and Han, Z. S., "Resonant Vibration Levels of a Mistuned Bladed Disk," *Journal of Vibration, Acoustics, Stress, and Reliability in Design,* Vol. 106, No. 2, 1984, pp. 211-217.

[23]MacBain, J. C., and Whaley, P. W., "Maximum Resonant Response of Mistuned Bladed Disks," *Journal of Vibration, Acoustics, Stress, and Reliability in Design,* Vol. 106, No. 2, 1984, pp. 218-233.

[24]Sogliero, G., and Srinivasan, A. V., "Fatigue Life Estimates of Mistuned Blades Via a Stochastic Approach," *AIAA Journal,* Vol. 18, No. 3, 1980, pp. 318-323.

[25]Huang, W., "Vibration of Some Structures with Periodic Random Parameters," *AIAA Journal,* Vol. 20, No. 7, 1982, pp. 1001-1008.

[26]Sinha, A., "Calculating the Statistics of Forced Response of a Mistuned Bladed Disk Assembly," *AIAA Journal,* Vol. 24, No. 11, 1986, pp. 1797-1801.

[27]Soong, T. T., and Bogdanoff, J. L., "On the Natural Frequencies of a Disordered Linear Chain of N Degrees of Freedom," *International Journal of Mechanical Sciences,* Vol. 5, 1963, pp. 237-265.

[28]Soong, T. T., and Bogdanoff, J. L., "On the Impulsive Admittance and Frequency Response of a Disordered Linear Chain of N-Degrees of Freedom," *International Journal of Mechanical Sciences,* Vol. 6, 1964, pp. 225-237.

[29]Lin, Y. K., and Yang, J. N., "Free Vibration of a Disordered Periodic Beam," *Journal of Applied Mechanics,* Vol. 41, No. 2, 1974, pp. 383-391.

[30]Yang, J. N., and Lin, Y. K., "Frequency Response Functions of a Disordered Periodic Beam," *Journal of Sound and Vibration,* Vol. 38, No. 3, 1975, pp. 317-340.

[31]Hamade, K. S., and Nikolaidis, E., "Probabilistic Vibration Analysis of Nearly Periodic Structures," *AIAA Journal,* Vol. 28, No. 4, 1989, pp. 676-684.

[32]Yong, Y., and Lin, Y. K., "Propagation of Decaying Waves in Periodic and Piecewise Periodic Structures of Finite Length," *Journal of Sound and Vibration,* Vol. 129, No. 2, 1989, pp. 99-118.

[33]Kennett, B. L. N., *Seismic Wave Propagation in Stratified Media,* Cambridge University Press, Cambridge, England, UK, 1983.

[34]Furstenberg, H., "Noncommuting Random Products," *Transactions of the American Mathematical Society,* Vol. 108, No. 3, 1963, pp. 377-428.

[35]Ziman, J. M., *Models of Disorder,* Cambridge University Press, Cambridge, England, UK, 1979.

[36]Hori, J., *Spectral Properties of Disordered Chains and Lattices,* Pergamon, Oxford, England, UK, 1968.